

Ab-initio calculations of magnetic and optical properties of 3x3 supercell of TiX₂ (X = S, Se and Te) compounds under the effect of externally applied electric field and strain

Aditya Dey

Department of Physics, Indian Institute of Technology Patna, Bihta Campus, India

The magnetic and optical properties of titanium dichalcogenide compounds, TiX₂ (X = S, Se and Te) have been calculated by first principles calculations using density functional theory (DFT) as implemented in SIESTA code. A 3x3 supercell of the compounds is taken in this study to be able to tune the properties obtained from the unit cell of these compounds. With magnetic states (ferromagnetic nature) as the attained ground state, spin polarized calculations are performed to obtain the mentioned properties. Further, with spin polarization into effect, external electric field (along z-direction) and biaxial strain (along x and y-directions) is employed to study their effect on these properties. The effect of biaxial strain on the geometry of the compounds is also studied. It is observed that the pristine supercell of the compounds possess a good amount of magnetic moment and this can be modulated using the applied field and strain. For the optical properties, polarized light along the z-direction (c axis) is used. These properties include the calculation of real & imaginary parts of dielectric function, absorption coefficient, reflectance, optical conductivity and refractive index in 0-25 eV energy range. Various modulations of these properties are observed including the blue-shifts and red-shifts of energies with highest peaks in the visible region and also shifting of energies to other regions of the electromagnetic spectrum. Hence, with the tunable magnetic and diverse optical properties, the compounds can be useful in the field of spintronics and in making various optical devices.

1. Introduction

In recent studies of material science and related areas over a span of few years, two-dimensional materials are in the limelight due to their variety of properties and remarkable applications in numerous fields. Of these materials, potential research is being carried out on layered transition metal dichalcogenides (TDMC) because of its anisotropic physical properties and strong covalent bound layers as well as their different technological applications^[1-6]. The titanium dichalcogenide compounds, TiX₂ (X = S, Se and Te) are one of the types of TDMC which has attracted a great amount of attention due to its wide range of applications^[7-13]. These compounds comprise of a covalently bonded Ti and X atoms in two-dimensional hexagonal planes. The planes are stacked together by chalcogen-chalcogen van der Waals interactions^[14-16]. These compounds have highly anisotropic physical properties. Therefore, significant changes in their properties can be made by foreign atoms or external factors.

TiX₂ crystallizes in 1T-type structure and with a space group *P-3m1* at room temperature and pressure^[17]. In earlier research works, these compounds have been studied both experimentally and theoretically including the study on their various properties. With an emphasis on the theoretical studies of these compounds, many researchers have dug into several properties like electronic, mechanical, magnetic, optical properties and so on^[18-21]. It is observed that all of these compounds possess a non-magnetic behaviour with 0.00 μ_B magnetic moment. For the optical properties, transmission spectra of TiS₂ and TiSe₂ are measured at liquid-helium temperature is measured with $E \perp c$ in the energy range 0.5–4 eV^[22]. Also the reflectivity of single crystals of TiS₂, TiSe₂ and TiTe₂ is measured with the electric field perpendicular to the hexagonal *c* axis in the energy range 1–12 eV^[23]. In addition to this, absorption spectra and reflectivity in other energy ranges has also

been reported ^[24-25]. Mentioning about the electronic properties, the previous reports show that there are many conflicts on their study as some works have reported that they behave as a semiconductor and at the same time some classify it as a semi-metal ^[26-28]. Hence, it remains as a matter of dispute as the property seems to change due to some marginal factors depending on different parameters. Also, some of reports show that people have studied the effect of strain or pressure on the band structures of these compounds in order to modulate the electronic properties ^[29-31].

Going through the available literature based on the study of these compounds, it can be found out that there is very scarce work done on the study of possible changes in their optical and magnetic properties which can be caused by external factors. So, in this article, a study has been performed to investigate the possible modulation and changes in the optical properties and magnetic moment of TiX_2 compounds via the effect of external electric field and strain, which is done theoretically using first principles calculation by density functional theory. In view of the optical properties, various optical characteristics of the compounds like absorption coefficient, reflectance, real and imaginary parts of dielectric function, refractive index and optical conductivity has been included in the study.

2. Computational details

The first principle calculations are performed using density functional theory (DFT) as implemented in the ab-initio package SIESTA ^[32-36]. The approach is based on an iterative solution of the Kohn–Sham equation. The generalized-gradient approximation (GGA) with the Perdew-Burke-Ernzerhof (PBE) form ^[37] is chosen for the exchange–correlation functional. A real space mesh cutoff of 300 Ry has been used for representing the charge density. Conjugate-gradient (CG) method ^[38] has been used to optimize the structures. Normconserving pseudopotentials in the fully nonlocal Kleinman–Bylander form have been considered for all the atoms ^[39]. A double- ζ polarized (DZP) basis set is used. Systems are considered to be relaxed only when the forces acting on all the atoms are less than $0.01 \text{ eV } \text{\AA}^{-1}$. A 3×3 supercell is taken for all the three compounds which are periodic along x and y directions (a & b axis) and vacuum space of at least 20 \AA is created along z direction to avoid any spurious interactions between the layers. The convergence for energy was chosen as 10^{-4} eV between two steps. Firstly, all the supercell structures of the compounds were optimized in both magnetic and non-magnetic states. Finding magnetic states as the ground state spin polarized self-consistent calculations were performed to employ the electric field along c axis and magnetic moment is obtained. Again using spin polarization, strain along a and b axis is applied and the structures are optimized followed by calculating the moment. Further, after applying external field and strain, optical properties were calculated for out of plane polarized light ($E||c$) for an energy range of $0\text{-}25 \text{ eV}$ and the direction of optical vector being (001). Optical calculations were carried out using $40 \times 40 \times 2$ optical mesh and optical broadening used is 0.1 eV . While performing the calculations of the mentioned properties under the effect of external factors and optimization of the structures as well, a $15 \times 15 \times 1$ k-point grid has been considered within the Monkhorst–Pack scheme ^[40] for each and every calculation.

3. Results and Discussions

3.1 Structural parameters

As stated previously, the main aim here is to study the effect of externally applied electric field and strain on the optical properties and magnetic moment of the TiX_2 compounds. For that, a 3×3 supercell of each of these compounds has been taken. The supercell is periodic only in two directions (a and b axis or x & y directions) and non-periodic along the c -axis. The structures have been optimized in non-magnetic states followed by optimization including spin polarization. Table 1 shows the comparison between total energies of both magnetic (M) and non-magnetic (NM) states.

From the table, it can be seen that the energy difference between the M and NM states ($E_M - E_{NM}$) is negative for all the structures of TiX_2 , indicating that the magnetic state is more stabilized over the non-magnetic state. Also as the stabilization energy is much higher than the room temperature energy (0.025 eV), M state seems to be robust in room temperature.

Compounds	E_{NM} (eV)	E_M (eV)	$E_M - E_{NM}$ (eV)	$a(\text{\AA})$	$b(\text{\AA})$	$c(\text{\AA})$	$\alpha(deg)$	$\beta(deg)$	$\gamma(deg)$
TiS₂	-6732.917	-6735.880	-2.963	9.23	9.22	20.59	89.74	89.96	120.00
TiSe₂	-6042.621	-6046.684	-4.063	9.27	9.28	21.05	89.99	90.05	120.04
TiT₂	-5042.268	-5047.297	-5.029	10.03	10.03	21.77	90.03	90.04	120.01

Table -1 Comparison of total energies of M and NM states and spin-polarized optimized structural parameters of TiX_2 compounds

A schematic model of the spin-polarized (M) optimized structure of these compounds is shown in Figure 1, which shows both the top view and side view of the supercell. It must be noted that the shown structure is same for all the compounds with slight changes in the lattice parameters, as recorded in Table 1. In one of the previously reported works on WSe_2 [41], it is observed that the spin-orbit interaction has almost no effect on the optical properties. So, in accordance to this report, in this study also, calculations have been performed including the spin orbit coupling (SOC), and similarly it is observed that there is very minor change in the results and so it is not reported in this article. While SOC is an essential factor for spin-polarized states in heavy metal compounds like of titanium, but the spin polarization emerging due to the magnetic moment of the atoms and the effect of SOC due to heavy metal (Ti in this case) plays a very minor role in the net magnetic moment of the compounds.

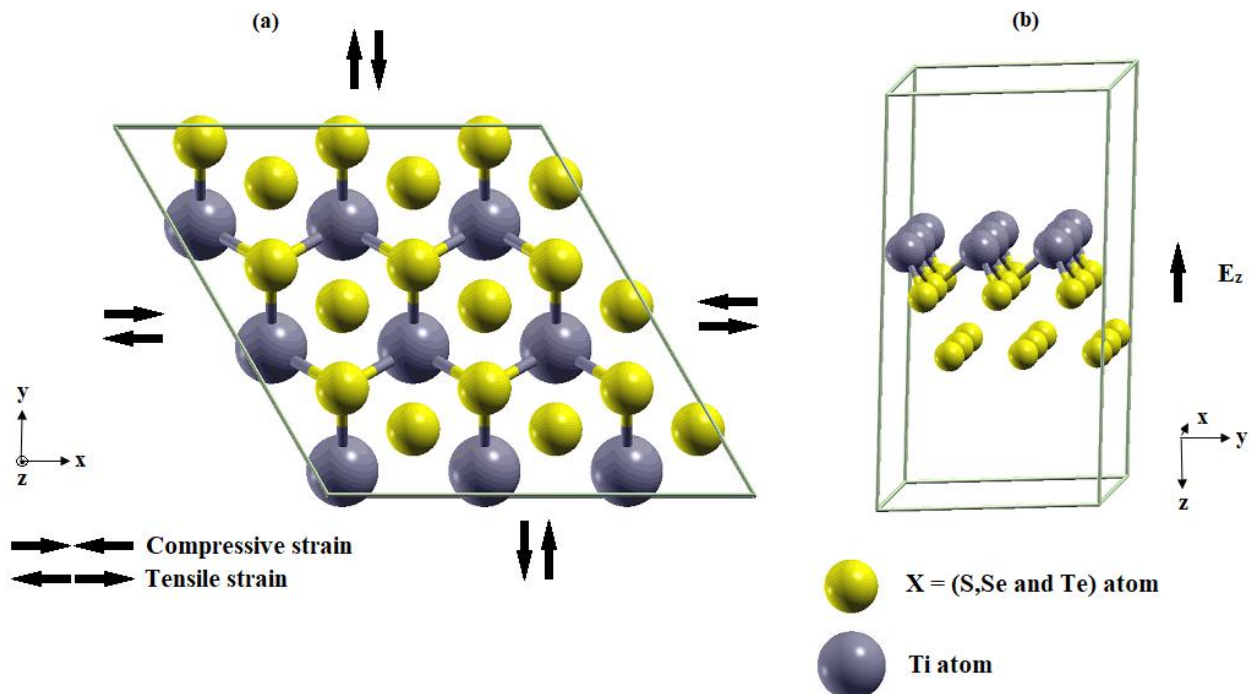


Figure 1 Ball and stick schematic diagram of TiX_2 compounds with (a) top view (b) side view including the directions of applied electric field and strain

The schematic above also shows the direction in which the externally applied electric field and biaxial strain is applied. Electric field is applied in the compounds in out of the plane or z direction (along c axis) which is denoted as E_z . The magnitude of field strength is varied from 2.5 V/nm to 10

V/nm. The optical properties as well as the magnetic moment is calculated and studied with different magnitudes of E_z . Self-consistent spin polarized calculation with particular magnitude of the field strength is performed to study the effect of E_z on the mentioned properties.

Strain is applied simultaneously along both a and b axis (x and y-directions) as shown in Figure 1. The biaxial strain applied is both tensile and compressive, denoted by plus (+) and minus (-) sign respectively. The amount of applied strain is $\pm 2\%$, $\pm 5\%$ and $\pm 10\%$. After freezing the strained lattices, the structures are optimized with spin polarization into effect and the geometric variations of the optimized structures are noted in Table 2. It can be seen that for all the compounds, Ti-X distance increases under tensile strain and decreases under compression. Whereas, for interlayer distance between S atoms, the previous trend is just reversed. This is in good agreement with a previous study done for strain in TiS_2 [42]. With increase in the atomic number of chalcogen atom, both $d_{\text{Ti-S}}$ and $h_{\text{S-S}}$ increases.

	TiS₂		TiSe₂		TiTe₂	
Strain (%)	$d_{\text{Ti-S}}$	$h_{\text{S-S}}$	$d_{\text{Ti-Se}}$	$h_{\text{S-S}}$	$d_{\text{Ti-Te}}$	$h_{\text{S-S}}$
Pristine 3X3 supercell	2.35	2.96	2.52	3.31	2.77	3.70
+ 2%	2.38	2.87	2.56	3.20	2.84	3.58
+ 5%	2.43	2.79	2.60	3.13	2.91	3.44
+ 10%	2.49	2.66	2.68	3.02	3.01	3.35
- 2%	2.31	3.04	2.41	3.43	2.72	3.77
- 5%	2.28	3.13	2.32	3.56	2.66	3.86
- 10%	2.25	3.21	2.19	3.68	2.60	3.98

Table 2 – Variations in geometry of the optimized structures under strain. $d_{\text{Ti-X}}$ denotes bond length between nearest Ti and X atom and $h_{\text{S-S}}$ denotes interlayer height between upper and lower S atomic planes

3.2 Magnetic properties

As can be found from the previous works, there is no magnetic moment present in the unit cell structure of the TiX_2 compounds. However, from this study it can be seen that a moment can be induced in these compounds by creating their supercell (refer Table 3 or Table 4), which is obtained because the structures show stabilization in the magnetic state (ferromagnetic arrangement). As can be seen from the tables, the obtained magnetic moment for pristine 3 X 3 supercell is 1.40 for TiS_2 , 1.91 for TiSe_2 and 2.13 μ_B for TiTe_2 , which is a considerable amount of moment. These moments are calculated per unit cell of the compounds. It is deduced by the expression, $\mu_{\text{TiX}_2} = \mu_{\text{Ti}} - 2(\mu_{\text{X}})$, where μ_{Ti} denotes the magnetic moment of Ti atom and μ_{X} denote that of chalcogen atoms (S, Se & Te atoms). μ_{TiX_2} denotes the total moment per unit cell of the compounds.

Also, this magnetic moment can be varied depending on the different magnitude of electric field and strain. Table 3 and Table 4 show the total magnetic moment and the local magnetic moment (per unit cell) as well, which is the individual contribution of Titanium and the chalcogen atom to the total moment, for all the compounds of TiS_2 , TiSe_2 and TiTe_2 with the applied field and strain respectively. It can be seen that the contribution to the total moment is majorly by the Ti atom, while the magnetic moment due to the chalcogen atoms is negligible. The electronic configuration of Ti atom is $[\text{Ar}] 3d^2 4s^2$ and that of S is $[\text{Ne}] 3s^2 3p^4$, Se is $[\text{Ar}] 3d^{10} 4s^2 4p^4$ and Te is $[\text{Kr}] 4d^{10} 5s^2 5p^4$. Hence, the magnetic contributions of Ti is mainly due to 3d orbital electrons and the somewhat negligible amount of moment due to S, Se and Te atoms is due to p orbital electrons. The reason for this is that for s- and p- valence electrons, the bonding-antibonding splitting is large which results in translating to a large band width due to strong orbital overlap in a solid. Formation of magnetic states is then unfavourable because large band width is equivalent to small density of

states. In contrast, the spatial extent of d and f orbitals is much smaller and also these orbitals only are enough localized and narrow as compared to other orbitals to give a high value to the exchange integrals between the spins, due to which they produce considerable amount of magnetic moment. Also, it is interesting to note that the magnetic moment contributed by the chalcogen atom is negative, which indicates that the chalcogen magnetic moment coming from the S 3p, Se 4p and Te 5p states is anti-parallel to the magnetic moment contributed by the Ti 3d states. Next, the effect of E_z and biaxial strain applied on these compounds is shown. It is observed that among the compounds, $TiTe_2$ has highest moment in pristine supercell as well as with the applied E_z and strain and TiS_2 has the lowest values.

Effect of electric field

Table 3 shows the variation of magnetic moment with each particular magnitude of applied field strength, which is applied in out of the plane direction. The attained magnetic behaviour for these compounds is of ferromagnetic nature.

Electric field (E_z)	TiS ₂			TiSe ₂			TiTe ₂		
	μ_{Ti}	μ_S	μ_{TiS_2}	μ_{Ti}	μ_{Se}	μ_{TiSe_2}	μ_{Ti}	μ_{Te}	μ_{TiTe_2}
Pristine 3X3 supercell	1.80	-0.20	1.40	2.29	-0.19	1.91	2.32	-0.09	2.13
2.5 V/nm	1.88	-0.11	1.66	2.39	-0.16	2.07	2.57	-0.05	2.47
5 V/nm	1.85	-0.10	1.65	2.36	-0.15	2.06	2.51	-0.03	2.45
7.5 V/nm	1.83	-0.11	1.61	2.35	-0.15	2.05	2.50	-0.03	2.44
10 V/nm	1.84	-0.13	1.58	2.33	-0.15	2.03	2.47	-0.02	2.43

Table -3 Magnetic moments of TiX_2 compounds with and without (pristine 3X3 supercell) E_z . (All moments are in Bohr magneton, (μ_B)).

Now, by application of electric field, it is observed that there is some amount of increase in the magnetic moment for all the compounds, with the highest increase in $TiTe_2$ with a total moment $2.47 \mu_B$, when the E_z magnitude is 2.5 V/nm and the same for TiS_2 is 1.66 and $2.07 \mu_B$ for $TiSe_2$. Again, when the magnitude of field strength E_z is increased, a trend of gradual decrease in the values of moment is recorded. It reduces to $1.58 \mu_B$ for TiS_2 , $2.03 \mu_B$ for $TiSe_2$ and $2.43 \mu_B$ for $TiTe_2$ at 10 V/nm. So, it is found that employing E_z , it is possible to increase the magnetic moment and even though the moment is decreasing with increasing E_z , the values are still greater than that of pristine TiX_2 supercell. Although the decrease is marginal, the trend is what must be noted. It is well known that by applying electric field to a compound or an element, there is subtle movement of the electron charge density. Hence it is possible that the electrons jump from one orbital to the other. Also, the partially filled d orbitals tend to show better ferromagnetism. Hence, in this case, in Ti atom, whose magnetism is generated by 3d states, the electric field causes movement of electron from s to d orbital, enabling it to show more magnetic moment and so we observe increase in local magnetic moment of Ti (μ_{Ti}). Along with Ti, though marginal, there is also shift of electrons in chalcogen atoms (μ_X). With increase in E_z , due to more variation in charge density in both atoms, net moment is getting reduced.

Effect of strain

Table 4 shows the modulation of magnetic moment of the TiX_2 compounds with the percentage of biaxial strain applied along a and b axis (+ indicates tensile and – indicates compressive strain). As stated earlier, the magnetic nature obtained is ferromagnetic.

Strain (%)	TiS ₂			TiSe ₂			TiTe ₂		
	μ_{Ti}	μ_S	μ_{TiS_2}	μ_{Ti}	μ_{Se}	μ_{TiSe_2}	μ_{Ti}	μ_{Te}	μ_{TiTe_2}
Pristine 3X3 supercell	1.80	-0.20	1.40	2.29	-0.38	1.91	2.32	-0.09	2.23
+ 2%	1.35	-0.13	1.09	1.42	-0.31	1.11	1.41	-0.31	1.10
+ 5%	0.62	-0.12	0.38	1.33	-0.34	0.99	1.22	-0.26	0.96
+ 10%	0.61	-0.14	0.33	1.02	-0.38	0.64	1.12	-0.35	0.77
- 2%	1.81	-0.18	1.45	1.97	-0.04	1.93	2.45	-0.04	2.41
- 5%	1.87	-0.16	1.55	2.32	-0.13	2.19	2.56	-0.09	2.47
- 10%	1.95	-0.14	1.67	2.44	-0.08	2.36	2.63	-0.10	2.53

Table – 4 Magnetic moments of TiX₂ compounds with and without (pristine 3X3 supercell) strain. (All moments are in Bohr magneton, (μ_B)).

For TiS₂, total moment decreases from 1.40 to 1.09 μ_B at +2% strain and tends to become feeble at +5% and +10% strain with values 0.38 and 0.33 μ_B respectively. Again it increases to 1.45 μ_B at -2% strain and climbs up to 1.55 and 1.67 μ_B at -5% & -10% respectively. Similarly, for TiSe₂, from 1.91 μ_B , it decreases to 1.11, 0.99 & 0.64 μ_B for +2%, +5% and +10% strain and increases to 1.93, 2.19 & 2.36 μ_B for -2%, -5% and -10% strain respectively. Again for TiTe₂, it decreases from 2.23 μ_B to 1.10, 0.96 & 0.77 μ_B for +2%, +5% and +10% strain & increases to 2.41, 2.47 & 2.53 μ_B for -2%, -5% and -10% strain respectively. So, it is seen that when tensile strain is applied, there is sudden decrease in the moment as compared to the unstrained structures, of both the local and total magnetic moment for all the compounds. Gradually, by increasing the percentage of strain, the total magnetic moment values become almost negligible. On the other hand, by employing compressive strain, there is a gradual increase in the values, and both the total and local magnetic moments increase with increasing the compressive strain. This is because due to tensile strain, the inter-atomic distance is increased and thus there is decrease in the exchange correlation or small overlap between the atomic orbitals. As a result, the ferromagnetic response gets suppressed, thus reducing the magnetic moment. With a similar explanation, as the inter-atomic distance decreases due to compressive strain, the magnetic moment gets enhanced. Thus, magnetic moment can be tuned by applying strain.

3.3 Optical properties

As stated earlier, the optical properties of all the compounds have been calculated for polarized light in out of the plane direction of the optical vector (001), that is, $E \parallel c$ axis in the energy range 0-25 eV. In view of this, different properties that have been investigated are absorption coefficient (α), reflectance (R), imaginary (ϵ_2) and real (ϵ_1) parts of dielectric constant, refractive index (n) and optical conductivity (σ). The complex dielectric function $\epsilon(\omega)$, can be expressed as $\epsilon(\omega) = \epsilon_1(\omega) + i\epsilon_2(\omega)$ and optical conductivity $\sigma(\omega)$ is calculated using $\epsilon(\omega) = \epsilon_0 + i\sigma(\omega) / \omega$, where ϵ_0 is the vacuum permittivity. The deduced properties are shown for TiS₂ only and the properties of the other two compounds are reported and compared further.

(a) Real and imaginary parts of dielectric function

The real and imaginary parts of the dielectric function are calculated for all the compounds. The pristine supercell of TiS₂ has maximum ϵ_1 value 7.21 at 1.52 eV and maximum $\epsilon_2 = 11.42$ at 1.57 eV (Figure 2). The same for TiSe₂ $\epsilon_1 = 10.72$ at 1.18 eV and $\epsilon_2 = 12.75$ at 1.31 eV and for TiTe₂, $\epsilon_1 = 13.08$ at 1.42 eV and $\epsilon_1 = 13.51$ at 1.81 eV (Table 5). For ϵ_1 , there are some dips in the amplitude in the range 1.6-2.2 eV, where it attains negative value indicating that there is plasmonic excitation in that range and most of the incident electromagnetic wave is reflected in this region. It can be

observed that peaks are seen in reflectance spectrum in the places where ϵ_1 becomes negative. Also, ϵ_1 becomes steady with increase in energy showing that it does not interact with energy photons (Figure 2(a)). A similar observation is noted for the other two compounds also. For TiS_2 , strong peaks of both ϵ_1 and ϵ_2 appear at near IR region (1.2 – 1.8 eV) whereas for TiSe_2 and TiTe_2 , it appears at both near IR and visible region (1.6 – 3.2 eV), which shows a contrasting behaviour of dielectric function with regard to electromagnetic spectrum. For all the compounds, peaks for ϵ_2 are observed in ~ 1.5 -2 eV range, which suggest that the compounds absorb electromagnetic waves in this range for this direction of polarization. At high energy (> 20 eV), ϵ_2 values vanishes, that tells there is no absorption of the compounds at very high frequency. The static dielectric constant is 5.13, 5.18 and 5.32 for TiS_2 , TiSe_2 & TiTe_2 respectively which shows that the value marginally increases with increasing atomic number of the chalcogen atom.

Effect of electric field – By employing E_z , a similar trend of gradual increase or decrease of the ϵ_1 & ϵ_2 values is found in the compounds. For TiS_2 , ϵ_1 & ϵ_2 increase to 8.16 & 14.18 at 1.38 and 1.43 eV respectively at 5 V/nm and then decrease further (Figure 2). In case of TiSe_2 , a drastic jump in the values is seen where ϵ_1 & ϵ_2 increase to 16.47 at 1.06 eV and 20.52 at 1.12 eV for 10 V/nm. For TiTe_2 , ϵ_1 & ϵ_2 decrease to 12.04 & 12.14 at 1.23 & 1.36 eV respectively at 10 V/nm. Also, there is no major shift in energies is observed with the application of electric field. The increase or decrease of values is related to the movement of electron density and electronic transitions caused by the effect of external field. Although, the changes in static dielectric constant is quite less for TiS_2 as compared to the other two compounds. For TiSe_2 & TiTe_2 , the values tend to increase gradually with increasing E_z (Table 5).

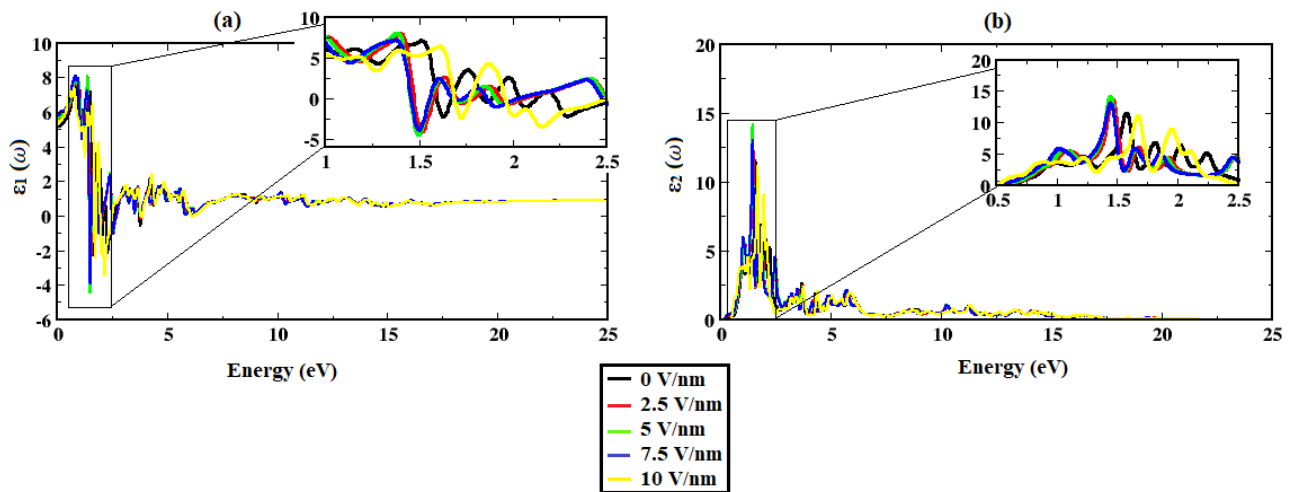


Figure 2 – (a) Real and (b) Imaginary values of dielectric function for TiS_2 under the effect of electric field. The peak regions are shown in the inset.

E_z (V/nm) & Strain (%)	TiS_2			TiSe_2			TiTe_2		
	Energy at max. peak (eV) ; ϵ_1	Energy at max. peak (eV) ; ϵ_2	Static dielectric const.	Energy at max. peak (eV) ; ϵ_1	Energy at max. peak (eV) ; ϵ_2	Static dielectric const.	Energy at max. peak (eV) ; ϵ_1	Energy at max. peak (eV) ; ϵ_2	Static dielectric const.
Pristine supercell	1.52; 7.21	1.57; 11.42	5.13	1.18; 10.72	1.31; 12.75	5.18	1.42; 13.08	1.81; 13.51	5.32
2.5 V/nm	1.41; 7.95	1.46; 13.76	5.52	1.15; 13.2	1.25; 16.45	5.57	1.34; 12.85	1.52; 13.09	5.70
5 V/nm	1.38; 8.16	1.43; 14.18	5.64	1.12; 14.54	1.19; 17.90	5.78	1.30; 12.54	1.51; 12.77	5.89
7.5 V/nm	1.37; 7.18	1.43; 13.06	5.81	1.11; 14.59	1.16; 19.23	6.01	1.27; 12.27	1.50; 12.05	6.06

10 V/nm	1.61; 6.38	1.67; 11.06	5.42	1.06; 16.47	1.12; 20.52	6.19	1.23; 12.04	1.36; 12.14	6.32
+2 %	2.68; 2.73	2.80; 1.45	2.20	0.02; 4.12	3.15; 1.39	4.08	0.62; 3.14	4.09; 1.47	2.93
+5 %	2.21; 2.48	4.68; 1.30	2.08	2.02; 2.82	4.19; 1.41	2.32	0.34; 3.53	3.57; 1.42	3.31
+10 %	2.19; 2.46	4.98; 1.35	2.10	2.08; 2.68	10.28; 1.27	2.11	1.24; 3.36	3.20; 1.38	2.70
-2 %	0.11; 5.38	3.56; 1.68	5.06	0.50; 3.29	4.36; 1.58	3.02	0.34; 3.94	1.60; 1.42	3.91
-5 %	3.36; 2.92	3.74; 1.58	5.40	0.00; 8.83	0.42; 3.47	8.83	0.00; 8.52	0.47; 3.37	8.52
-10 %	1.26; 3.13	5.27; 1.51	2.73	0.00; 9.98	0.28; 3.65	9.98	0.02; 9.15	0.14; 3.44	9.15

Table -5 Values of static dielectric constant and real & imaginary values of dielectric function including energies with peak positions under the effect of E_z and strain for all the compounds.

Effect of strain – With the different amount of applied biaxial strain, it is seen that there are changes in the values of dielectric function along with shift in energies which varies with the direction of strain and the compound also. For TiS_2 , both the ϵ_1 & ϵ_2 values are decreased to a great extent for both directions of strain (Figure 3). The energies for ϵ_2 values in both the strain are blue shifted & for ϵ_1 , blue-shifts are present in tensile strain and red shifts are seen in -2% & -10% strain. The static dielectric constant is reduced in tensile strain & for -10% strains. From Table 5, one can observe that similar to TiS_2 , for TiSe_2 & TiTe_2 also there are mixed variations of energy shifts and ϵ_1 & ϵ_2 values, however it must be noted that both ϵ_1 & ϵ_2 values have decreased with respect to that in pristine supercell with the application of strain. For tensile strain in TiSe_2 & TiTe_2 , static dielectric constant decreases alike TiS_2 and also for compressive strain of -2 % but the value increases for -5% & -10% strain.

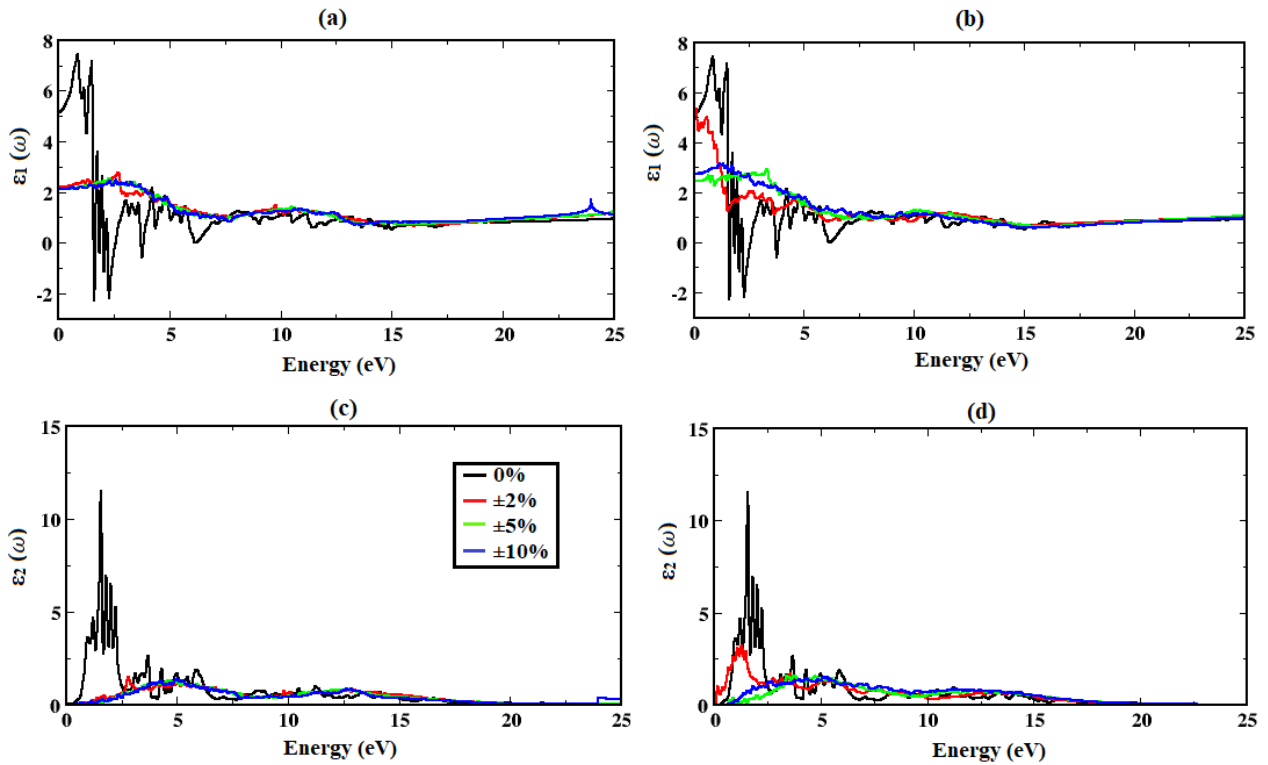


Figure – 3 Real and imaginary values of dielectric function for TiS_2 under (a, c) tensile and (b, d) compressive strain. The peak regions are shown in the inset.

(b) Absorption coefficient and Reflectance

The pristine supercell of TiS_2 , that is, without any applied field or strain, shows that there is strong absorption at 6.06 eV and 11.37 eV, with the highest peak at 11.37 eV with $\alpha = 5.4 \times 10^5 \text{ cm}^{-1}$ (Figure 4(a) or 5(a,b) & Table 6). Both the peaks show that they are in the Ultraviolet light region (3.9 – 14 eV photon energy), which means there are low electron losses and high absorbance in this

region and can be attributed to the interband transitions, similar to as stated for ϵ_2 . Similarly, the pristine TiSe₂ supercell show strong absorption at 10.34 and 13.24 eV, with maximum value of $\alpha = 10.4 \times 10^5 \text{ cm}^{-1}$ at 13.24 eV and for TiTe₂ highest peaks are attained at 8.75 & 13.82 eV with maximum absorption of $\alpha = 6.5 \times 10^5 \text{ cm}^{-1}$ at 13.82 eV. So, as similar to TiS₂, these two compounds also exhibit absorption in the UV region.

The reflectance of pristine TiS₂ supercell from Figure 4(b) or 5(c, d) & that of TiSe₂ and TiTe₂ from Table 7 shows that these compounds show moderate amount of reflectivity. For TiS₂, highest reflectance attained is 0.47 at 2.29 eV and that of TiSe₂ & TiTe₂ is 0.43 at 1.39 and 0.61 at 2.38 eV. The range of peaks for TiS₂ and TiTe₂ is in visible region & in near infrared region for TiTe₂. So, ~50-60 % reflection of light in visible and infrared region is observed for these compounds and hence it shows they reflect more than half of the incident light.

Effect of Electric field – By applying different magnitudes of E_z , there is a gradual increase in the absorption coefficient observed for all the compounds (Table 6). For TiS₂, α increases maximum to $5.7 \times 10^5 \text{ cm}^{-1}$ at 11.32 eV energy with field strength of 10 V/nm. Similarly for TiSe₂ and TiTe₂, at the same field strength, α increases to 10.7×10^5 and $8.3 \times 10^5 \text{ cm}^{-1}$ at 13.84 eV & 13.98 eV respectively. The range of energies with highest peaks observed for all the values of E_z shows they all lay in the UV region only for all the compounds. However, when the energy value with the highest peak is considered, some blue-shifts and red-shifts are observed. For TiS₂, there is a red-shift of ~5.5 eV with E_z values ranging from 2.5 – 7.5 V/nm. Again in TiSe₂, minor blue-shifts of 0.1-0.6 eV for all values of E_z and in TiTe₂, red shifts of ~5 eV is present for E_z range of 5-10 V/nm. The reflectivity is somewhat tuned by increasing E_z . It has gradually ascended to 0.59 and 0.57 at 2.22 and 1.19 eV for TiS₂ & TiSe₂ respectively and descended to 0.42 at 2.25 eV for TiTe₂ for field strength of 10 V/nm (Table 7). For TiS₂, the reflectance region is shifted to near IR from visible region at 2.5-7.5 V/nm causing a red-shift of ~0.7 eV. In TiSe₂ and TiTe₂ the region is same with red-shifts of ~0.1-0.2 eV and ~0.1 eV respectively.

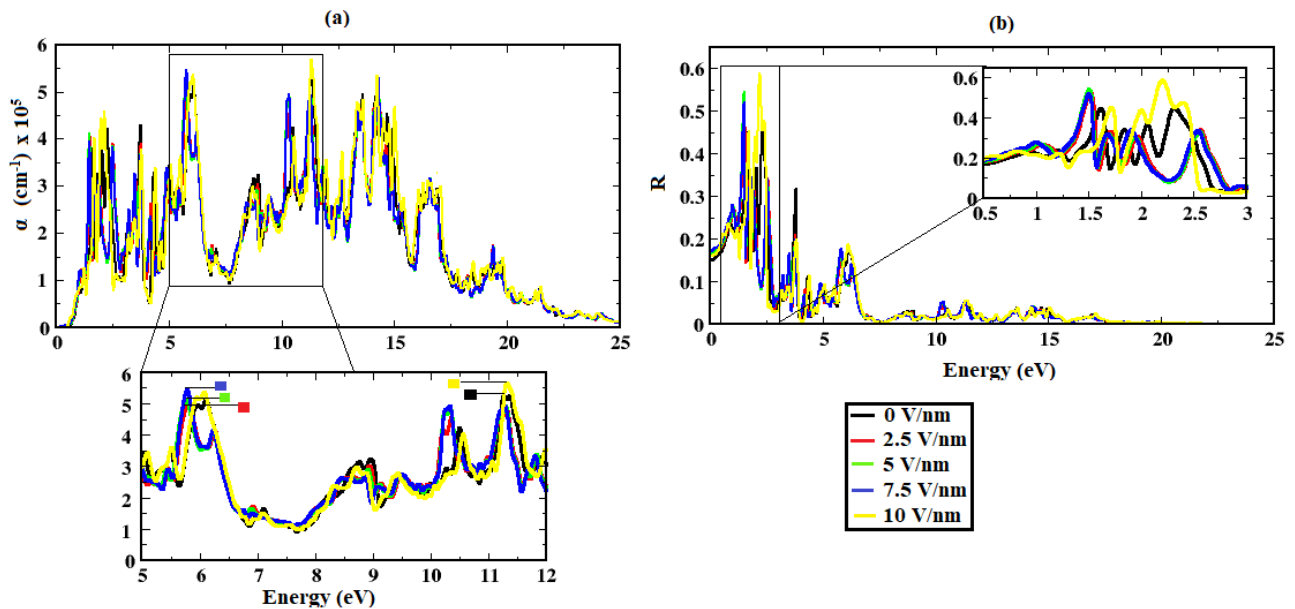


Figure 4 – (a) Absorption coefficient and (b) Reflectance of TiS₂ under the effect of electric field. The peak regions are shown in the inset. The peaks of each field strength is shown in respective colour in inset of fig 2(a)

E_z (V/nm) & Strain (%)	TiS₂			TiSe₂			TiTe₂		
	Energies with highest peaks (eV)	Energy at max. peak (eV)	Maximum α (cm ⁻¹) x 10 ⁵	Energies with highest peaks (eV)	Energy at max. peak (eV)	Maximum α (cm ⁻¹) x 10 ⁵	Energies with highest peaks (eV)	Energy at maximum peak (eV)	Maximum α (cm ⁻¹) x 10 ⁵
Pristine supercell	6.06, 11.37	11.37	5.0	10.34, 13.22	13.22	10.4	8.75, 13.82	13.82	6.5
2.5 V/nm	5.81, 11.18	5.81	5.1	10.42, 13.31	13.31	10.4	8.69, 13.89	13.89	6.4
5 V/nm	5.73, 11.23	5.73	5.2	10.44, 13.52	13.52	10.5	8.73, 13.91	8.73	6.6
7.5 V/nm	5.75, 11.29	5.75	5.5	10.46, 13.68	13.68	10.6	8.77, 13.92	8.77	7.9
10 V/nm	6.06, 11.35	11.35	5.7	10.49, 13.86	13.86	10.7	8.82, 13.95	8.82	8.3
+2 %	12.8-15.0	13.69	4.9	12.7-14.2	13.68	4.5	9.7-11.0	10.57	4.0
+5 %	12.5-13.5	13.05	4.8	13.3-13.8	13.74	4.1	8.5-10.8	9.59	4.5
+10 %	12.7-13.5	12.83	5.2	9.8-11.0	10.24	5.6	8.8-10.6	9.56	4.9
-2 %	13.0-15.0	14.21	4.9	13.0-14.5	13.19	4.9	10.4-12.0	11.04	4.7
-5 %	12.2-14.5	14.23	5.1	13.2-15.0	14.18	5.5	11.9-13.5	12.55	5.5
-10 %	12.0-14.6	14.41	5.5	7.5-9.3	8.71	9.6	11.5-13.3	12.96	5.8

Table -6 Energies with peak positions and absorption coefficient values under the effect of E_z and strain for all the compounds. ('-' represents range of energies with highest peak & ',' represents particular energies of high peaks)

Effect of strain – Both the tensile & compressive strain tends to alter the absorption and there are no particular sharp peaks observed. The α value increases with increasing the amount of strain (Table 6). For TiS₂, α increases to 5.2 & 5.5 x 10⁵ cm⁻¹ at 12.83 & 14.41 eV energy peaks for +10 % and -10 % strain respectively. For same amounts of tensile and compressive strain, again for TiSe₂ and TiTe₂, α increases to 5.6 & 9.6 x 10⁵ cm⁻¹ at 10.24 & 8.71 eV and 4.9 & 5.8 x 10⁵ cm⁻¹ at 9.56 & 12.96 eV respectively. The recorded energies are at UV region, as similar to pristine supercell. Again, for TiS₂, there is a blue-shift of ~1.5-2.3 eV, for TiSe₂, there is blue shift of ~0.5-1 eV and red shift of ~3-4.5 eV and for TiTe₂ there is only red shift of ~1-4 eV. The increase in absorption and the shifts is seen due to excitation of phonons by increasing both tensile & compressive applied strain.

The reflectance values from Table 7 shows that there are some sharp peaks for some values of applied strain, where there is shift in the energy. However, despite such jumps, it can be seen that the reflectance values are almost negligible in most of the cases. For TiS₂, R value ranges from 0.06-0.16 for both the directions of strain. For TiSe₂ and TiTe₂, it ranges from 0.06-0.26 & 0.08-0.27 respectively for both tensile & compressive strain. Also, there is blue-shift of ~0.5-2.5 eV and red-shift of ~1 eV for TiS₂. In case of TiSe₂, there is blue shift of ~1 eV and red-shift of ~1.2-1.3 eV and for TiTe₂ there is only red shift of ~1-2.3 eV. So, with the applied strain, it can be seen that reflectivity is drastically reduced.

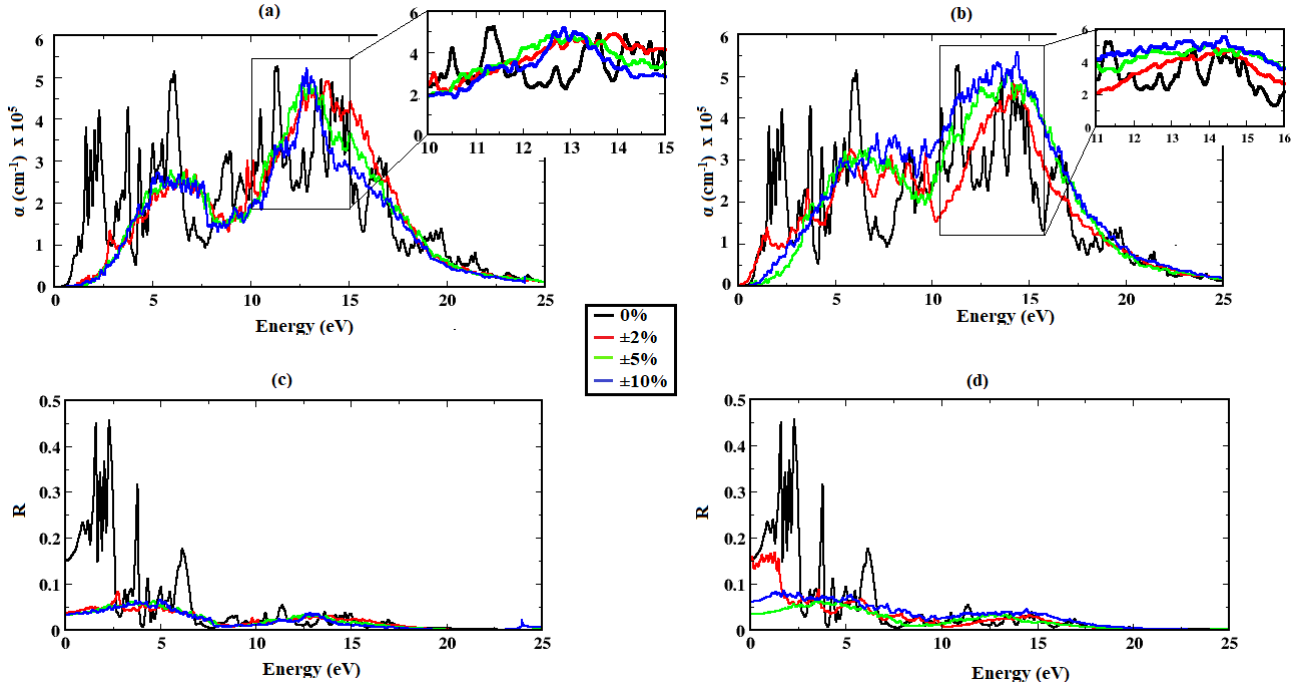


Figure – 5 Absorption coefficient and Reflectance of TiS_2 under (a, c) tensile and (b, d) compressive strain. The peak regions are shown in the inset.

E_z (V/nm) & Strain (%)	TiS_2			TiSe_2			TiTe_2		
	Energies with highest peaks (eV)	Energy at max. peak (eV)	Maximum R	Energies with highest peaks (eV)	Energy at max. peak (eV)	Maximum R	Energies with highest peaks (eV)	Energy at maximum peak (eV)	Maximum R
Pristine supercell	1.63, 2.29	2.29	0.47	1.39, 1.71	1.39	0.43	2.38, 3.40	2.38	0.61
2.5 V/nm	1.59, 2.62	1.59	0.52	1.30, 1.86	1.30	0.48	2.31, 3.30	2.31	0.55
5 V/nm	1.57, 2.60	1.57	0.53	1.28, 1.83	1.28	0.52	2.28, 3.27	2.28	0.50
7.5 V/nm	1.49, 2.59	1.49	0.51	1.23, 1.75	1.23	0.55	2.26, 3.17	2.26	0.45
10 V/nm	2.22, 2.41	2.22	0.59	1.19, 1.71	1.19	0.57	2.25, 3.15	2.25	0.42
+2 %	2.5-2.8	2.78	0.08	0.06-0.19	0.15	0.12	1.1-1.5	1.40	0.08
+5 %	4.5-4.8	4.65	0.06	2.37-4.14	3.34	0.07	0.3-0.6	0.40	0.09
+10 %	4.7-5.1	5.01	0.06	2.48, 10.27	2.48	0.06	1.28, 1.48	1.28	0.10
-2 %	0.6-1.4	1.26	0.16	0.57-0.1	0.94	0.10	0.4-0.5	0.46	0.11
-5 %	3.3-3.8	3.43	0.06	0.02	0.02	0.24	0.06	0.06	0.23
-10 %	1.3-5.2	1.77	0.08	0.11, 8.80	0.11	0.26	0.1-0.2	0.11	0.27

Table -7 Energies with peak positions and reflectance values under the effect of E_z and strain for all the compounds. ('-' represents range of energies with highest peak & ',' represents particular energies of high peaks)

(c) Optical conductivity and refractive index

The maximum optical conductivity for all the pristine supercell structures is nearly equal with TiTe_2 having the highest value of $\sigma = 2.81 \times 10^5 \Omega\text{m}^{-1}$. Also, the energies with maximum peaks lie in the near IR region for TiS_2 & TiSe_2 but some peaks are also present in the visible region for TiTe_2 (Table 8). However, some peaks of comparatively lesser σ values were seen in the visible region also in case of TiS_2 and TiSe_2 . With increase in photon energy, conductivity seems to get vanished. The range of peaks attained for conductivity is aligned to the absorption spectra.

The static refractive index of pristine supercell of all the compounds is almost same. But the maximum value of n attained is 2.26, 3.41 and 3.76 for TiS_2 , TiSe_2 & TiTe_2 respectively, with the energies at the highest peak being almost equal for them. The refractive index is > 1 due to the fact that as photons enter a material they are slowed down by the interaction with electrons and further, the more photons are slowed down travelling via the material, more is the refractive index. The peaks with high energies are mainly seen in the near IR region only for all the compounds (Table 9).

Effect of electric field – With the electric field, for TiS_2 and TiSe_2 the σ value increases and for TiTe_2 , it is decreased. In case of TiS_2 , σ increases maximum to $2.74 \times 10^5 \Omega\text{m}^{-1}$ at 1.44 eV for 5 V/nm (Figure 6(a)) and to $3.10 \times 10^5 \Omega\text{m}^{-1}$ at 1.13 eV for 10 V/nm in case of TiSe_2 and decreases to $2.46 \times 10^5 \Omega\text{m}^{-1}$ at 1.51 eV for 7.5 V/nm in case of TiTe_2 . Also, there is very minor energy shifts for TiS_2 and TiSe_2 . For TiTe_2 , there is no shift in energy peaks is observed until $E_z = 10$ V/nm, where a blue shift of ~ 7 eV is seen. However, having a look at the energies with highest peaks on applying the external field, it is observed that high peaks of σ values are present in both near IR & visible as well as UV regions.

Electric field seems to modulate the refractive index for all the compounds. The static value of n is gradually increased by applying E_z in all the cases, with increased value 2.40, 2.48 & 2.51 for TiS_2 , TiSe_2 & TiTe_2 respectively at 10 V/nm. Whereas, with increasing strength of E_z the maximum value of n increases abruptly for TiS_2 and smoothly for TiSe_2 . On the other hand, it decreases smoothly for TiTe_2 (Table 6). The region of highest energy peaks are also the same, which lies in the near IR regime. This also shows that there is no major energy shifts. The increase in static n is due to the increase in electron density caused by E_z and any factor increasing the electron density also increase the refractive index. With increase in photon energy, the trend is altered because of electronic excitations.

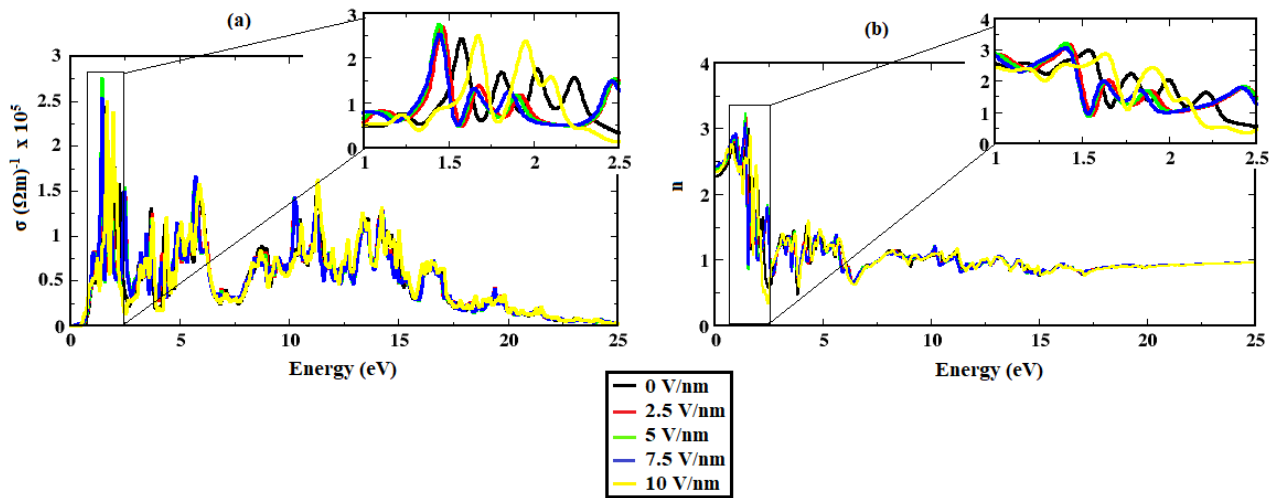


Figure – 6 (a) Optical conductivity and (b) Refractive index of TiS_2 under the effect of electric field. The peak regions are shown in the inset.

E_z (V/nm) & Strain (%)	TiS_2			TiSe_2			TiTe_2		
	Energies with highest peaks (eV)	Energy at max. peak (eV)	Maximum σ (Ωm^{-1}) $\times 10^5$	Energies with highest peaks (eV)	Energy at max. peak (eV)	Maximum σ (Ωm^{-1}) $\times 10^5$	Energies with highest peaks (eV)	Energy at maximum peak (eV)	Maximum σ (Ωm^{-1}) $\times 10^5$
Pristine supercell	1.57, 1.65	1.57	2.44	1.31, 1.71	1.31	2.28	1.51, 2.15	1.51	2.81
2.5 V/nm	1.46, 2.46	1.46	2.69	1.24, 1.67	1.24	2.71	1.51, 2.05	1.51	2.70
5 V/nm	1.44, 2.46	1.44	2.74	1.20, 1.67	1.20	2.89	1.51, 8.71	1.51	2.61
7.5 V/nm	1.43, 2.45	1.43	2.52	1.16, 1.66	1.16	3.02	1.51, 8.74	1.51	2.46
10 V/nm	1.68, 1.95	1.68	2.50	1.13, 1.69	1.13	3.10	1.39, 8.77	8.77	2.72

+2 %	11.6-14.0	12.99	1.34	12.5-14.5	13.71	1.19	9.0-10.6	9.20	1.44
+5 %	11.6-13.5	12.52	1.39	11.5-13.7	11.95	1.08	9.40, 11.38	9.40	1.13
+10 %	11.5-13.2	12.68	1.44	10.24, 12.18	10.24	1.75	9.47, 10.56	9.47	1.28
-2 %	12.7-15.0	13.52	1.12	11.7-14.2	13.14	1.28	8.5-11.3	11.07	1.24
-5 %	11.2-15.0	12.52	1.34	13.4-14.5	13.99	1.45	7.17, 11.95	7.17	1.46
-10 %	10.5-15.0	13.17	1.36	8.05, 8.70	8.70	1.51	8.95, 12.10	8.95	1.98

Table -8 Energies with peak positions and optical conductivity values under the effect of E_z and strain for all the compounds. ('-' represents range of energies with highest peak & ',' represents particular energies of high peaks)

Effect of strain – The application of both tensile and compressive strain shows that the σ value is reduced by stretching the lattice in case of all the compounds. Some large amount of blue-shifts is also seen (Table 8). For the compounds, σ value is almost same for strain applied along both directions and for TiS_2 , it reduces to 1.34 & $1.12 \times 10^5 \Omega\text{m}^{-1}$ for +2% & -2% respectively. For TiSe_2 , σ is decreased to 1.08 & $1.28 \times 10^5 \Omega\text{m}^{-1}$ for +5% & -2% respectively and for TiTe_2 , for same amount of strain, σ is reduced to 1.13 & $1.24 \times 10^5 \Omega\text{m}^{-1}$. For both the direction of strain, there is a blue-shift of ~ 12 eV, ~ 7.5 - 12.5 eV and ~ 6 - 9.5 eV in case of TiS_2 , TiSe_2 and TiTe_2 respectively. Similar to what observed with applied E_z , peaks is observed near IR, visible as well as UV regions.

For refractive index, the value of static n as well as maximum value of n is decreased in case of tensile strain (Table 9). For TiS_2 , there is also some blue-shifts in energy (~ 1 eV) is seen for tensile strain and red-shifts of 0.75 - 1 eV is seen in case of TiTe_2 . For TiSe_2 , blue-shift of ~ 1 eV is observed for +5% and +10% strain & a red-shift of ~ 1 eV for +2% strain. When compressive strain is applied, for TiS_2 , both the static and maximum value of n is reduced but less as compared to tensile strain. A similar observation is recorded for maximum n for the other two compounds, but for both TiSe_2 and TiTe_2 , static n increases for -5% & -10% strain. Also, applying compressive strain, we see similar values of static and maximum n , which also causes energy shifts to mid-IR region.

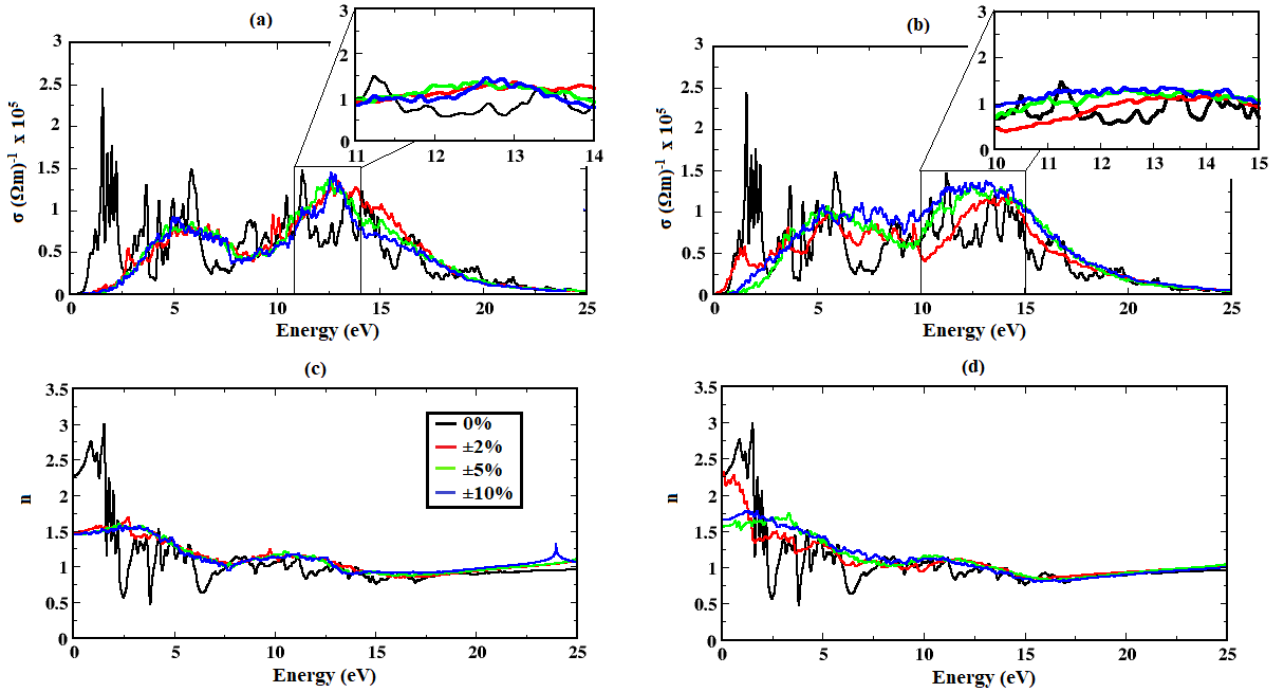


Figure – 7 Optical conductivity and Refractive index of TiS_2 under (a, c) tensile and (b, d) compressive strain. The peak regions are shown in the inset.

E_z (V/nm) & Strain (%)	TiS ₂			TiSe ₂			TiTe ₂		
	Energy at max. peak (eV)	Maximum n	Static refract. Index n	Energy at max. peak (eV)	Maximum n	Static refract. Index n	Energy at max. peak (eV)	Maximum n	Static refract. Index n
Pristine supercell	1.53	2.99	2.26	1.24	3.41	2.27	1.48	3.76	2.30
2.5 V/nm	1.42	3.20	2.32	1.17	3.81	2.35	1.35	3.69	2.38
5 V/nm	1.40	3.22	2.34	1.13	3.99	2.39	1.31	3.67	2.42
7.5 V/nm	1.39	3.06	2.37	1.10	4.17	2.45	1.26	3.64	2.46
10 V/nm	1.63	3.01	2.40	1.07	4.28	2.48	1.24	3.59	2.51
+2 %	2.72	1.68	1.47	0.13	2.04	2.01	0.86	1.77	1.71
+5 %	2.27	1.59	1.44	1.96	1.68	1.51	0.35	1.87	1.82
+10 %	2.32	1.56	1.43	2.15	1.64	1.45	1.27	1.84	1.64
-2 %	0.02	2.25	2.25	0.56	1.81	1.74	0.36	1.99	1.97
-5 %	3.33	1.74	1.55	0.00	2.98	2.98	0.00	2.91	2.91
-10 %	1.74	1.78	1.64	0.00	3.15	3.15	0.00	3.22	3.22

Table -9 Values of static and maximum refractive index including energies with peak positions under the effect of E_z and strain for all the compounds.

The increase in some of the optical properties observed due to E_z is mainly because of increased electron density movement causing interband transitions starting from lower photon energy to higher photon energy. All the interband transitions are essentially due to the p orbital of the X (X = S, Se & Te) atoms moving to the d orbital of the Ti atoms. When both tensile and compressive is applied, it is observed that although there is a shift in the energy with the maximum value of the properties, there are very less sharp peaks obtained and thus the shift in energy has not occurred swiftly, rather a gradual rise in the peaks is seen. This shows hindrance in the interband transitions which occurs because electron correlation plays a major role for the strained structures and the electrons are localized around the atoms, thus becoming less drifting. So, it can be seen a reduction in the obtained values of properties with strain. However, for compressive strain, due to reduction in Ti-X distance (Table 2), there is redistribution of electrons which may enable orbital excitations. Hence, some sharp peaks and increase in values of properties can be seen for compressive strain.

Conclusion

In summary, the magnetic and optical properties of TiX₂ (X= S, Se and Te) compounds have been calculated using ab-initio calculations including the effect of externally applied electric field and biaxial strain. A 3x3 supercell of the compounds has been taken to study the properties. Optimization of the structures including magnetic and non-magnetic states has been performed and it is found that the magnetic state (ferromagnetic nature) is more stable. So using spin polarized calculations, the properties of the pristine supercells is investigated. It is observed that a considerable amount of magnetic moment is attained for the supercell structures. Also, the compounds show good response to the deduced optical properties, which is calculated using polarized light along z-direction. Further, electric field (along z-direction) and biaxial tensile and compressive strain (along x and y-direction) is employed on the structures. With electric field, it is seen that there is increase in the magnetic moment as well as the calculated optical properties, which is observed due to the increase in orbital transitions of electrons in the compounds. On the other hand, for applied tensile strain, the calculated values of both the properties are seen to reduce. For compressive strain, magnetic moment increases to a good extent and some of the optical properties (static n & static ϵ and α in some of the cases) are also seen to increase with increasing the strain. But for most of the optical properties are observed to decrease under applied compressive strain. Some major shifts in energies with highest peaks of these properties are also seen when strain is applied, where the peaks shift from one region of the electromagnetic spectrum to other.

Hence, applying these external factors, we can attain quite good amount of magnetic moment and even be able to tune it, which shows these compounds can be widely used in the field of spintronics. Also, with the factors into effect, we can obtain modulating optical properties and especially the attained high refractive index and dielectric constant can find applications in optoelectronic devices.

References

- [1] A. E. Maniadaki, *et.al.*, "Strain engineering of electronic properties of transition metal dichalcogenide monolayers," *Solid State Communications*, vol. **227**, 2016.
- [2] J. Kang, *et.al.*, "Computational Study of Metal Contacts to Monolayer Transition-Metal Dichalcogenide Semiconductors," *Phys. Rev. X*, Vols. **4**, 031005, 2014.
- [3] Riley Gatensby, *et.al.*, "Controlled synthesis of transition metal dichalcogenide thin films for electronic applications," *Applied Surface Science*, vol. **297**, 2014.
- [4] L. M. Xie, "Two-dimensional transition metal dichalcogenide alloys: preparation, characterization and applications," *Nanoscale*, no. **24**, 2015.
- [5] Y. Hu, *et.al.*, "Two-dimensional transition metal dichalcogenide nanomaterials for biosensing applications," *Mater. Chem. Front*, vol. **1**, 2017.
- [6] X. Li, *et.al.*, "Recent Advances in Synthesis and Biomedical Applications of Two-Dimensional Transition Metal Dichalcogenide Nanosheets," *Small*, vol. **13**, no. 5, 2017.
- [7] M. Parvaz, *et.al.*, "Synthesis of TiS₂ nanodiscs for supercapacitor application," in *AIP Conference Proceedings*, 2018.
- [8] X. Sun, *et.al.*, "Layered TiS₂ Positive Electrode for Mg Batteries," *ACS Energy Lett.*, vol. **1**, 2016.
- [9] P. Li, *et.al.*, "Electrochemical potassium/lithium-ion intercalation into TiSe₂: Kinetics and mechanism," *Energy Storage Materials*, vol. **16**, 2019.
- [10] F. Levy-Bertrand, *et.al.*, "Puzzling evidence for surface superconductivity in the layered dichalcogenide Cu(10%)TiSe₂," *Physica C: Superconductivity and its Applications*, vol. **523**, 2016.
- [11] P. Chen, *et.al.*, "Emergence of charge density waves and a pseudogap in single-layer TiTe₂," *Nature communications*, vol. **8**, 2017.
- [12] R. C. Xiao, *et.al.*, "Manipulating superconductivity of 1T-TiTe₂ by high pressure," *Journal of Materials Chemistry C*, vol. **17**, 2017.
- [13] Y. Liu, *et.al.*, "TiS₂ nanoplates: A high-rate and stable electrode material for sodium ion batteries," *Nano Energy*, vol. **20**, 2016.
- [14] V. V. Ivanovskaya, *et.al.*, "Electronic structure of titanium disulfide nanostructures: Monolayers, nanostripes, and nanotubes," *Semiconductors*, vol. **39**, 2005.
- [15] Z. Vydrova, *et.al.*, "Three-dimensional momentum-resolved electronic structure of 1T-TiSe₂: A combined soft-x-ray photoemission and density functional theory study," *Phys. Rev. B*, Vols. **91**, 235129, 2015.
- [16] V. N. Strocov, *et.al.*, "Three-dimensional band structure of layered TiTe₂: Photoemission final-state effects," *Phys. Rev. B*, Vols. **74**, 195125, 2006.
- [17] H. El-Kouch, *et.al.*, "Electronic and Optical Properties of TiS₂ Determined from Generalized Gradient Approximation Study," *Chinese Phys. Lett.*, Vols. **32**, 096102, 2015.
- [18] A. H. R. and S. Auluck, "Electronic and optical properties of the 1T phases of TiS₂, TiSe₂, and TiTe₂," *PHYSICAL REVIEW B*, vol. **68**, 2003.
- [19] T. Lorenz, *et.al.*, "Theoretical Study of the Mechanical Behavior of Individual TiS₂ and MoS₂ Nanotubes," *J. Phys. Chem. C*, vol. **116**, 2012.
- [20] M. Inoue, *et.al.*, "The electronic and magnetic properties of the 3d transition metal intercalates of TiS₂," *Advances in Physics*, vol. **38**, no. 5, 1989.
- [21] Y. Tazuke, *et.al.*, "Magnetic properties of MxTiSe₂ (M = Mn, Fe, Co)," *phys. stat. sol.*, vol. 3, no. 8, 2006.

- [22] A. R. Beal, *et.al.*, "Transmission spectra of some transition metal dichalcogenides," *Journal of Physics C: Solid State Physics*, vol. **5**, 1972.
- [23] H. P. H. and W. Y. Liang, "Vacuum ultraviolet reflectivity spectra of the disulphides and diselenides of titanium, zirconium and hafnium," *Journal of Physics C: Solid State Physics*, vol. **10**, 1977.
- [24] S. C. B. and W. Y. Liang, "Symmetry dependence of optical transitions in group 4B transition metal dichalcogenides," *Journal of Physics C: Solid State Physics*, vol. **15**, 1982.
- [25] L. Baldassarre, *et.al.*, "Photoacoustic reflectivity spectra of titanium dichalcogenides," *Optics Communications*, vol. **71**, 1989.
- [26] C. M. Fang, *et.al.*, "Bulk and surface electronic structure of 1T-TiS₂ and 1T-TiSe₂," *Phys. Rev. B*, Vols. **56**, 4455, 1997.
- [27] H. D. Ozaydin, *et.al.*, "Electronic and Magnetic Properties of 1T-TiSe₂ Nanoribbons," *arXiv*, vol. 1509.03467, 2018.
- [28] J. C. E. Rasch, *et.al.*, "1T-TiSe₂: Semimetal or Semiconductor?," *Phys. Rev. Lett.*, Vols. **101**, 237602, 2008.
- [29] A. Samanta, *et.al.*, "Strain-induced electronic phase transition and strong enhancement of thermopower of TiS₂," *Phys. Rev. B*, Vols. **90**, 174301, 2014.
- [30] G. A. Benesh, *et.al.*, "The pressure dependences of TiS₂ and TiSe₂ band structures," *Journal of Physics C: Solid State Physics*, vol. **18**, 1985.
- [31] Q. Zhang, *et.al.*, "Series of topological phase transitions in TiTe₂ under strain," *Phys. Rev. B*, Vols. **88**, 155317, 2013.
- [32] J. M. Soler, *et.al.*, "The SIESTA method for ab initio order-N materials simulation," *Journal of Physics: Condensed Matter*, vol. **14**, 2002.
- [33] N. T. and J. L. Martins, "Efficient pseudopotentials for plane-wave calculations," *Phys. Rev. B*, Vols. **43**, 8861, 1991.
- [34] W. Kohn and L. J. Sham, "Self-Consistent Equations Including Exchange and Correlation Effects," *Phys. Rev.*, Vols. **140**, A1133, 1965.
- [35] D. M. C. and B. J. Alder, "Ground State of the Electron Gas by a Stochastic Method," *Phys. Rev. Lett.*, Vols. **45**, 566, 1980.
- [36] P. Ordejón, *et.al.*, "Self-consistent order-N density-functional calculations for very large systems," *Phys. Rev. B*, Vols. **53**, R10441(R), 1996.
- [37] J. P. Perdew, *et.al.*, "Generalized Gradient Approximation Made Simple," *Phys. Rev. Lett.*, Vols. **77**, 3865, 1996.
- [38] W. Press, *et.al.*, *New Numerical Recipes*, New York: Cambridge University Press, 1986.
- [39] L. K. and D. M. Bylander, "Efficacious Form for Model Pseudopotentials," *Phys. Rev. Lett.*, Vols. **48**, 1425, 1982.
- [41] S. Sharma, *et.al.*, "Optical properties and band structure of 2H-WSe₂," *Phys. Rev. B*, vol. **60**, 8610, 1999
- [42] Chengyong Xu, *et.al.*, "Strain induced semimetal-to-semiconductor transition and indirect-to-direct band gap transition in monolayer 1T-TiS₂," *RSC Adv.*, vol. **5**, 83876, 2015